

Evaluating Cold Atmospheric Plasma for Endoscope Decontamination: Feasibility and Impact Analysis on PTFE Surfaces

Juliette Zveny,^{a,*} Antoine Remy,^b Pierre Nickmilder,^c Alain Delchambre,^b Antoine Nonclercq,^b Philippe Leclère,^c & François Reniers^a

^aChemistry of Surfaces, Interfaces, and Nanomaterials (ChemSIN), Université Libre de Bruxelles, Faculty of Sciences, Brussels, Belgium; ^bBio-Electro- and Mechanical Systems (BEAMS), Biomed Group, Ecole Polytechnique de Bruxelles, Brussels, Belgium; ^cLaboratory for Physics of Nanomaterials and Energy (LPNE), Research Institute in Materials Science and Engineering, University of Mons (UMONS), Mons, Belgium

*Address all correspondence to: Juliette Zveny, Chemistry of Surfaces, Interfaces, and Nanomaterials (ChemSIN), Université Libre de Bruxelles, Faculty of Sciences, Brussels, Belgium; Tel.: +32 2 650 31 44, E-mail: juliette.zveny@ulb.be

ABSTRACT: Plasma decontamination of medical devices has garnered significant attention in recent years. This paper explores the feasibility of decontaminating endoscopes, which are extensively used in hospitals for minimally invasive procedures but are a leading cause of nosocomial infections due to inadequate cleaning. Cold atmospheric plasma offers a promising solution by potentially providing an effective and easily implemented decontamination method. However, improper use could damage the endoscope. A setup was developed to mimic the internal channel of endoscopes, and a dielectric barrier discharge (DBD) plasma device was designed, capable of reaching the entirety of a 1.5 m polytetrafluoroethylene (PTFE) tube. The impact of the plasma on the endoscope's internal channel was analyzed. Extensive surface studies of the PTFE tube (atomic force microscopy, X-ray photoelectron spectroscopy, and water contact angle) and gas analysis of the post-plasma (Fourier-transform infrared spectroscopy) treatment were conducted. These studies enabled the determination of the treatment conditions (gas, power, duration) that affect the PTFE tube and an assessment of the extent of the impact.

KEY WORDS: cold plasma, endoscope decontamination, PTFE

I. INTRODUCTION

Currently, endoscopes undergo cleaning and decontamination through well-established procedures involving enzymatic solutions and brushing the devices' internal channels.¹ However, endoscopes often retain bacterial contaminants even after thorough cleaning.² Those remaining contaminations of endoscopes increase the risk of cross-contamination between patients. Indeed, endoscopes are reported to be the medical device causing the most surgery-related infections by the US Center for Disease Control.³ Moreover, little to no information is known on the impact of the current cleaning process on endoscopes and the damages it may entail.

The persistent contamination challenges lie in the complexity of the endoscope structure, making some parts difficult to reach and properly clean. Additionally, the electronic part of the devices makes them incompatible with autoclaving at high

temperatures.³ Among the various decontamination methods, plasma offers a potential solution by providing efficient and thorough decontamination of the internal channels of endoscopes. Indeed, plasma is gaining attention for its antibacterial and antimicrobial properties.⁴

Cold atmospheric plasma (CAP), with known antibacterial properties, is already being explored in several biomedical applications, with two main purposes: plasma used for cleaning and decontamination of medical devices and material⁵⁻⁷ and plasma used to treat patients conditions, with ongoing studies exploring its application in diverse diseases^{8,9} or wounds treatment.¹⁰ This study falls into the former. CAP is emerging as a promising method for cleaning and decontaminating hard-to-reach areas in tubular structures, such as endoscopes.^{11,12} Polytetrafluoroethylene (PTFE), commonly used in endoscopes for its antifouling properties, can benefit from CAP treatment.

PTFE is a versatile polymer used in many applications due to its exceptional properties, including high thermal and chemical resistivity, a low friction coefficient, and low surface tension.¹³ These characteristics make PTFE an ideal material for various uses, particularly where non-adhesive and antifouling properties are advantageous. Examples of such applications include PTFE membranes for wastewater ultrafiltration, marine structure protection, and vascular grafts.¹⁴⁻¹⁶ The effectiveness of PTFE in these applications relies heavily on maintaining its surface properties. However, even PTFE is susceptible to fouling over time, especially when in contact with wet materials, necessitating periodic deep cleaning and decontamination.¹⁷ Endoscopes are a prime example of such applications, with their internal channels made of PTFE and biofouling garnered on their surfaces over time.

The inertness of PTFE, which is a desirable attribute, may also be compromised under plasma treatment. Research shows that plasma can significantly affect the chemical and topographical properties of PTFE surfaces.¹⁸⁻²¹ The effects of plasma on PTFE depend on various parameters, including the type of gas used, the power and the frequency applied, as well as the energy of the plasma species.^{11,19,22} For instance, oxygen-containing plasmas tend to erode the amorphous phase of PTFE, while noble gas plasmas can cause surface sputtering with no preferential attack on the crystalline or amorphous phases.²³ These interactions can cause mass loss²⁴ and alter surface roughness.²⁵ The latter has been shown to increase the adherence of biofouling.²⁶ The wettability of the polymer is also affected, which can impact biofouling and, more specifically, biofilm formation and adherence. However, the extent of this impact is still under debate.²⁶

Given these potential effects, this study examines the impact of plasma treatment on PTFE in a tubular system, designed to mimic the structure of endoscopes. PTFE tubes are prevalent in numerous applications, from medical devices to high-pressure water systems, making this research broadly applicable,²⁷⁻²⁹ and this system could theoretically be applied to all of them. This study investigates the viability of using CAP for endoscope decontamination as well as the impact of different plasma parameters on the surface modifications of PTFE, aiming to balance effective decontamination with minimal adverse effects on the material (the decontamination treatment is discussed in a separate work).³⁰

II. MATERIALS AND METHODS

A. Setup

To ignite the plasma inside the entire tube, the work of Bastin et al. and Thulliez et al.^{31,32} was repurposed. They developed a dielectric barrier discharge (DBD) in a PTFE tube that generates a plasma jet 2 meters away from the high voltage (HV) input and minimizes the losses along the tube. On the contrary, the objective here is to utilize the losses to our advantage, and so to maximize the plasma occurring inside the tube.

As shown on Fig. 1, a setup mimicking the working channel of an endoscope as closely as possible while remaining easily analyzed was built. It consists of a 1.5-m-long PTFE tube provided by Chemlab Analytical, with an internal diameter of 3 mm and 1.5 mm thickness (3 mm ID \times 5 mm OD), acting as the endoscope's working channel. A PVC tube (8 mm ID and 12 mm OD) surrounds the PTFE tube and is encased by a metallic mesh, serving as the electronic housing and the electrical ground. Together, the apparatus mimics the principal electrical and structural characteristics of an endoscope tubular structure.

The plasma device is made of a 45 mm long stainless steel (SS) tube (1/4-inch 316L from Swagelok), acting as a gas pass-through and a high voltage connection. The PTFE tube is gas-tightly connected to the SS tube downstream. A 1.5-m-long by 0.3-mm-wide copper wire is attached inside the SS tube and serves as the powered electrode running inside the entire PTFE tube. To generate plasma in a controlled atmosphere, a flowmeter (MV-302, Bronkhorst) injects a controlled flow of gas into the tubes. Multiple vector gases (helium, nitrogen, and argon) are used in this study, mixed or not with reactive gases like air, oxygen, and water. The total gas flow for all experiments is 1.5 L/min. The different gases are provided by Air Liquide with purity over 99.99% (Alphagaz 1). In the

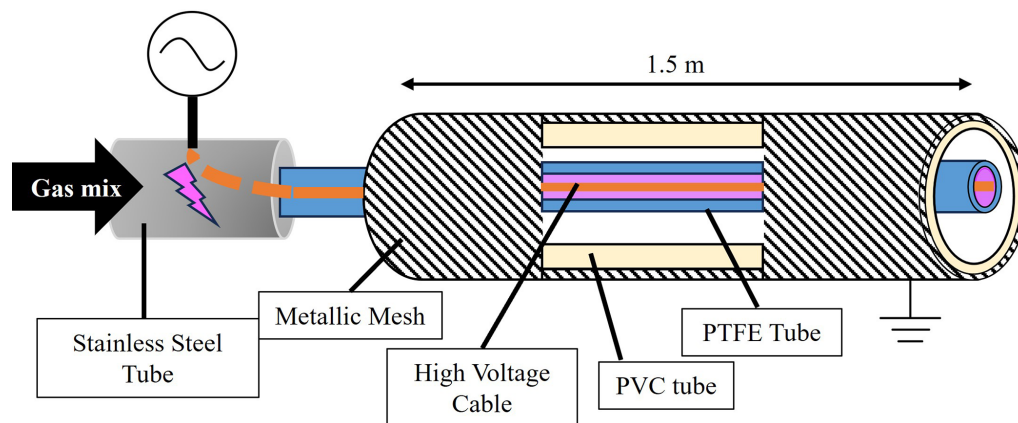


FIG. 1: Setup of the plasma generator with the display mimicking the endoscope

case of water vapor addition, a bubbler filled with deionized water was used to charge the vector gas with humidity. The bubbler was positioned upstream from the SS tube.

The high-voltage AC power was provided by a G10S-V AFS generator, which allows for power and frequency control. The powers used in this study vary from 5 watts to 35 watts. The AC power was used in continuous as well as in milli-pulsed mode. The milli-pulsed mode is characterized by alternance of ON (i.e., with power applied) and OFF (i.e., without power applied) periods, both at the millisecond scale. Several OFF times were used with a fixed ON time of 1 ms; OFF times varied between 1, 3, 5, and 9 ms.

B. Plasma Analysis

1. High-Speed Camera

A high-speed camera (Photron FASTCAM NOVA S6) equipped with a Tamron SP AF 90 mm F/2.8 Di Macro 1:1 lens was used to visualize the plasma characteristics (luminosity, filamentary or homogenous aspect). The images were recorded at 1000 fps. To better visualize the discharge inside the tube apparatus, a cutout in the PVC tube was realized, and the discharge was observed through the metallic mesh and the PTFE tube, both essential to the discharge characteristics.

2. Oscilloscope

The electrical properties of the plasma were monitored with a high-voltage probe (Tektronix P6015A) and recorded on an oscilloscope (500 MHz, Tektronix DPO 3032). The total electrical power was measured and displayed by the AFS generator.

C. Gas Analysis

1. Fourier Transform Infrared Spectrometry (FTIR)

The analysis of the gases produced by the discharge was made by infrared absorption spectroscopy using a fourier transform infrared (FTIR) spectrometer (Bruker Vertex 70 V) with a set of external mirrors. The infrared beam goes through a 20-cm-length homemade gas cell with zinc selenide windows. The spectral range analyzed is from 700 to 4400 cm^{-1} . Spectra are taken every 5 seconds with a resolution of 0.5 cm^{-1} . The produced molecules were identified with the associated bands and quantified with reference cross-section spectra from Hitran.³³ The concentration of those species in the gas stream is obtained using the Beer-Lambert law (see equation) at specific wave numbers, specifically chosen to avoid as much overlaps with other species bands as possible.

$$C = A \frac{\rho}{L.C_s}$$

where C is the concentration of the species in part per million by volume (ppm-v); A the absorbance measured at the wavenumber of interest; ρ the gas density: 2.46×10^{13} molecule.ppm-v⁻¹; L the optical path of the IR beam in cm; and C_s the absorption cross-section in cm² molecule⁻¹. The wavenumber and the associated cross-sections chosen for analysis of the different species are presented in Table 1. The vibrational band chosen for COF₂ is ν_1 , at 1944 cm⁻¹.

D. Surface Analysis

Surface analysis of narrow tubular structures like the PTFE tube is a challenge. Therefore, flat surfaces were used for analysis, as represented in Fig. 2. Instead of tubes, 0.1 mm thick PTFE films (Goodfellow) cut into 1 × 2 cm rectangular pieces were used, rolled up, and inserted into the PTFE tube at approximately 1 cm from the end of the tube. The film is treated in the same conditions as the rest of the tube. After the plasma treatment, those films are unrolled, and the flattened treated part is analyzed using the following methods.

1. X-Ray Photoelectron Spectroscopy (XPS)

The PTFE surfaces were analyzed by XPS. The analysis was performed by a VersaProbe II photoelectron spectrometer (PhysicalElectronics) with a monochromatic Al K α X-ray source (1486.6 eV). Full survey and C 1s high-resolution spectra were performed on all samples with a 200 μ m diameter analysis spots. The pass energies for the full survey and the high-resolution spectra were 93.9 eV and 23.5 eV, respectively, with energy resolution of 0.8 eV and 0.1 eV.

The spectra were treated with CasaXPS. Full survey spectra were used to determine the average atomic concentration. The sensitivity factors used were 1 for C 1s, 2.93 for O 1s, and 4.43 for F 1s. Three different positions were analyzed on each sample and then the atomic composition of all spectra was averaged.

2. Water Contact Angle (WCA)

The wettability of the surfaces was measured using a WCA analysis. A Krüss “DSA100” goniometer was used in static mode, and the angle was calculated with the help of “drop

TABLE 1: Absorption cross-section (C_s) from Hitran³³ and wavenumber of absorption (W_n) used for qualitative and quantitative measurements

Species	HF	COF ₂	CF ₄
C_s (10 ⁻¹⁸ cm ² molecule ⁻¹)	1.14	1.20	68.86
W_n (cm ⁻¹)	4039	1944	1283

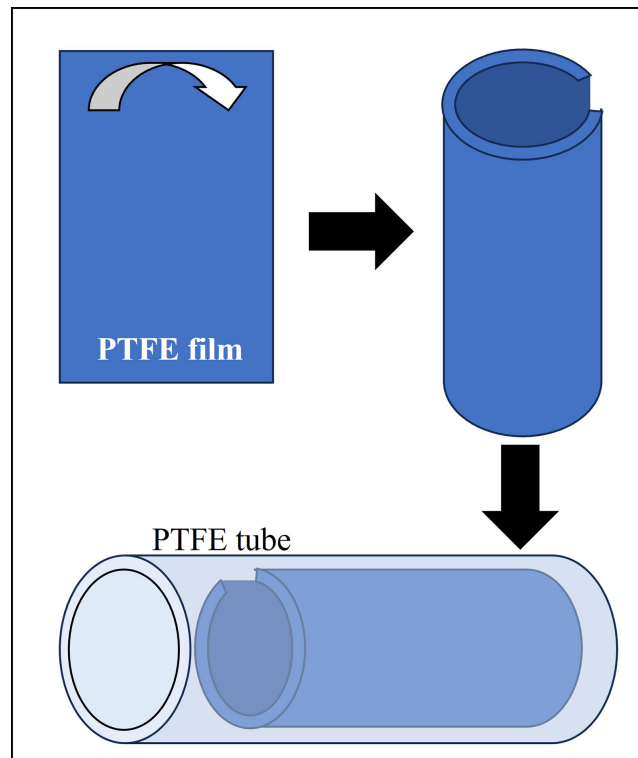


FIG. 2: Schematic representation of the insertion of a 1×2 cm PTFE film in a PTFE tube to obtain flat surfaces for surface analysis techniques

shape analysis” software. Three droplets of deionized water ($3 \mu\text{L}$) were deposited on the surface of each sample, and the angle values were averaged.

3. Atomic Force Microscopy (AFM)

The morphology of the surfaces of PTFE samples was analyzed by AFM in air. The microscope used is a Bruker dimension icon. The images were acquired in tapping mode with a resolution of 512×512 pixels and a scan size of $15 \times 15 \mu\text{m}$. The tip used are Bruker RTESPA 300 with a resonance frequency of about 300 kHz and a stiffness of about 40 N/m. The root mean square average surface roughness (R_q) was determined each sample using Nanoscope Analysis 3.0 software (Bruker).

III. RESULTS AND DISCUSSION

The result section is divided into three parts. 1) The successful ignition of plasma in a 1.5-m-long tube, backed up by high-speed camera images as well as electrical power measurements. The results show here that some parameters, such as the discharge

voltage, are crucial elements to ignite the plasma in the tube. 2) The analysis of the gases exiting the PTFE tube using FTIR. The detected fluorine species are correlated to the damage of the PTFE tube. 3) The surface analysis of the surfaces of the PTFE film after plasma treatment. Those analyses are done with AFM, XPS, and WCA.

A. Plasma in a Tube

Research on plasma in tubes usually uses a plasma jet configuration. Several goals can be pursued with these configurations. Bastin et al. and Thulliez et al. used it to provide a plasma plume at the end of a 2 m tube for non-invasive surgical purposes.^{32,33} Lu et al. aimed to decontaminate pipes with a helium plasma jet. Bhatt et al. targeted endoscope decontamination and used a plasma jet configuration.³⁴ While some success was achieved by those researchers with their respective goals, a different approach was undertaken in this study, utilizing dielectric barrier discharge (DBD) instead. The objective was to maximize plasma generation within the tube rather than focusing on plasma generation at the tube's end. Such a configuration distributes homogeneously the plasma's power on the tube's inner surface. Sato et al. pursued a similar goal, trying to clean catheters.³⁵ The main difference between this DBD setup and a plasma jet setup, resides in the electrical ground. In this case, the electrical ground is around a central powered electrode, much like a cylindrical DBD.

A polymeric tube, like those used in endoscopes, can be used directly as the dielectric barrier of the DBD, with the wire going through the PTFE tube and a metallic mesh wrapped around the tube. Fortunately, regular endoscopes have metallic wiring around their operating channel that can be used as grounding, and metallic wire can easily be placed inside the channel.

Every part of the electrical circuit of the DBD is critical to obtain plasma that ignites inside the entirety of the tube. Figure 3 illustrates the importance of the electrical circuit. Using a copper wire to transport the high voltage all the way inside the tube, as well as a metallic mesh around the tube acting as the ground electrode (Fig. 3A), allows a DBD plasma to be ignited inside the PTFE tube. When the metallic mesh is not connected to the ground (Fig. 3B), the plasma still ignites in the entire tube but with a lower intensity than when connected to the ground. Also, a small plasma jet at the end of the tube is observed. The last case (Fig. 3C) has the high voltage input only to the SS tube, with no copper wire inside the tube. In this case, the plasma stays localized next to the SS tube, with upstream and downstream jets observed.

The electrical circuit of the setup influences the extent of the plasma. The required conditions to create an intense and homogenous plasma inside of the entirety of the tube are obtained when the copper wire is connected to HV and the surrounding mesh is connected to the electrical ground. This configuration should be used for a homogenous treatment and fast decontamination of the tube. It is, therefore, used for the rest of this work.

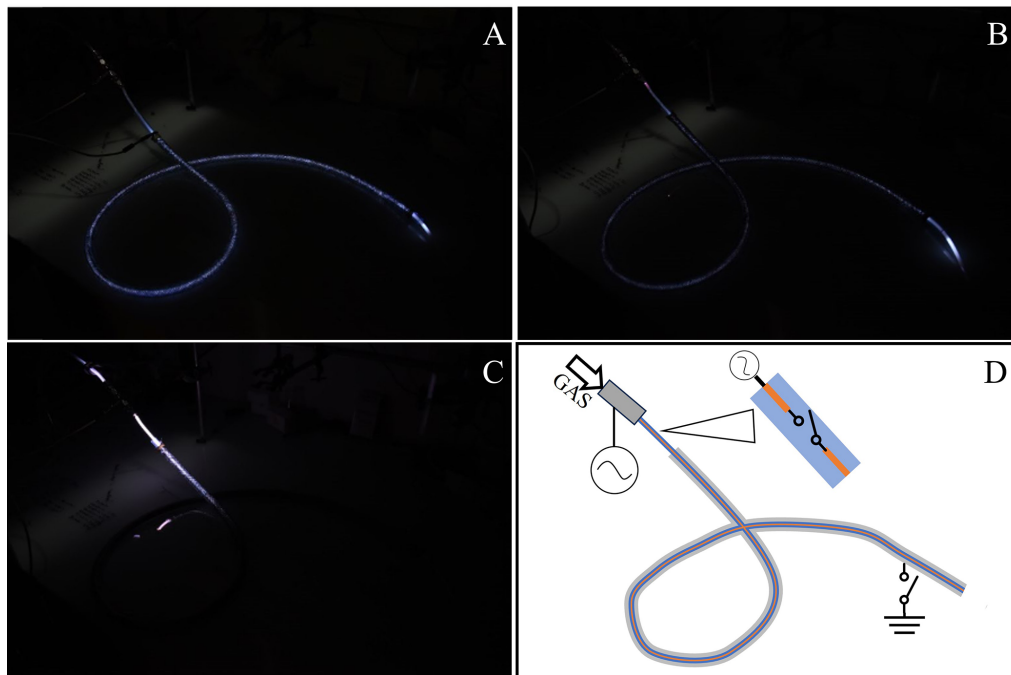


FIG. 3: Pictures of the setup with different electrical compositions in a 15 W Ar/H₂O plasma. (A) High voltage connected to the copper wire and ground connected to the metallic mesh. (B) High voltage connected to the copper wire and no ground. (C) High voltage applied to the SS tube. (D) Schematic illustration of the setup and its electrical connections.

In Fig. 4, the importance of electrical parameters is highlighted. By tweaking simple parameters such as the voltage, the appearance of the plasma is greatly affected, making it more, or less homogenous and modifying the volume it occupies.

A high-speed camera was used to examine the discharge's distribution within the tube. Figure 4 illustrates the influence of voltage on the discharge, showing that, for a fixed power, higher voltages allow the plasma to fill a larger volume inside the tube. The generator's power is fixed at 15 W with an ON time of 1 ms, while varying the OFF time between 0 and 9 ms. The resulting plasma voltage ranged from 5 kV in continuous mode (0 ms) to 17 kV at 9 ms OFF. As observed from Fig. 4A to 4D, higher voltage discharge enabled a more homogeneous treatment of the entire tube surface. With a regular AC, the applied voltage, at 5053 (\pm 61) V is too low to ignite plasma along the entire tube, and the plasma is only present directly next to the copper wire, the electrode. With pulsed current, an increase in the luminosity of the plasma is observed, which is linked to the increase in voltage. For OFF times of 1 and 4 ms, with a voltage of respectively 6694 (\pm 260) V and 11877 (\pm 202) V, the plasma presents a higher luminosity but is still restricted around the wire. At a pulse of 9 ms OFF, with 17879 (\pm 120) V, the plasma seems to reach the entirety of the tube, although

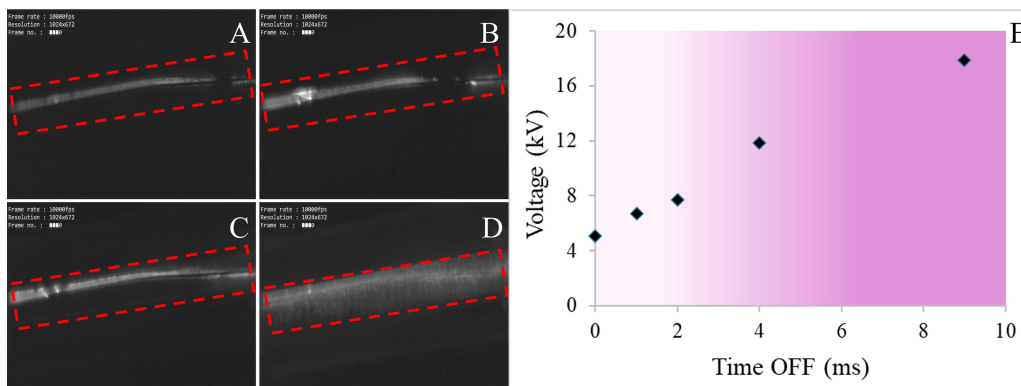


FIG. 4: Variation of the filamentary properties of the plasma with the increased voltage in a 15 W Ar/H₂O plasma. (A) AC. (B) Pulsed current (1 ms ON/1 ms OFF). (C) Pulsed current (1 ms ON/4 ms OFF). (D) Pulsed current (1 ms ON/9 ms OFF). (E) Graph of the voltage of the discharge with the increased time OFF and fixed time ON (1 ms).

at variable intensity. Using pulse mode, the voltage increased almost five times and ignited luminous plasma in the tube.

Figure 4 also shows that the plasma is confined into the PTFE tube, even at high voltage. That highlights the importance of vector gas to plasma ignition. Indeed, in this case, argon flows only inside the PTFE tube, leaving the PVC tube filled with air.

B. Gas Analysis

Figure 5 (left) shows the FTIR spectra of the exiting gases for an Ar/O₂ discharge at 15 W in continuous mode (0 ms OFF time). Fluorine-containing molecules were observed and measured in all tested plasma conditions (Fig. 5, right). HF and COF₂ were identified as well as, in some cases, CF₄. Other species, like CO₂, CO, and water, are also observed, depending on the plasma parameters, but they are irrelevant to the study. The

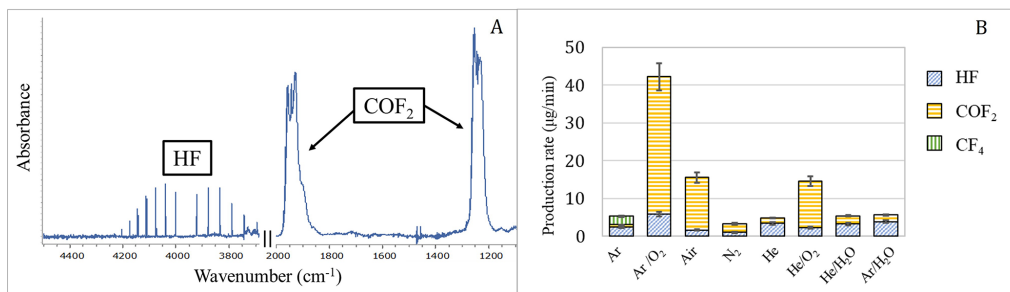


FIG. 5: (A) IR spectrum of exiting gas with HF and COF₂. (B) Tracking of the degradation of the PTFE tube depending on the gas mix used. Plasma at 15 W.

focus is on the fluorinated species as those are produced by the interaction of the plasma and PTFE and allow tracking of the deterioration of the PTFE surface. The concentration of those species in the gas cell was calculated in ppm-v and then converted into grams of species ejected from the tube per minute of plasma treatment ($\mu\text{g}/\text{min}$).

Multiple gases at a gas flow of 1.5 L/min and applied power of 15 W were tested. Important variations in the production of fluorinated molecules were observed. Plasma in pure noble gas (Ar and He) produced around 5 $\mu\text{g}/\text{min}$ of fluorinated molecules, with the notable production of CF_4 for pure argon. Ar/O_2 plasma stands out with the highest production rate at 42 $\mu\text{g}/\text{min}$. Ar/O_2 plasma is a mix of 97% argon and 3% oxygen for a total flow of 1.5 L/min. Same for He/O_2 . Those two gas mixes, as well as air, present the highest degradation rates with 15 $\mu\text{g}/\text{min}$ for air and He/O_2 . Oxygen seems to play an important role in the destruction of the polymer. This property of oxygenated plasma has already been observed in other works, although in different configurations. The oxygen radical is believed to be responsible for that degradation.²³ $\text{Ar}/\text{H}_2\text{O}$ plasma is a water-saturated flow of argon obtained from argon passing through a bubbler full of deionized water. $\text{He}/\text{H}_2\text{O}$ is the same with helium. Those showed similar deterioration rates, with respectively 5.4 and 5.5 $\mu\text{g}/\text{min}$ of fluorinated species ejected.

A focus was placed on Ar/O_2 and $\text{Ar}/\text{H}_2\text{O}$ plasma, as both are regularly found in decontamination treatments.³⁶ A variation of the plasma power has a significant influence on PTFE degradation. As seen in Fig. 6, Ar/O_2 plasma has the most destructive properties with a higher production rate of fluorine-containing compounds than the $\text{Ar}/\text{H}_2\text{O}$ plasma. After a rapid increase of production rate between 5 W, with 11 $\mu\text{g}/\text{min}$, and

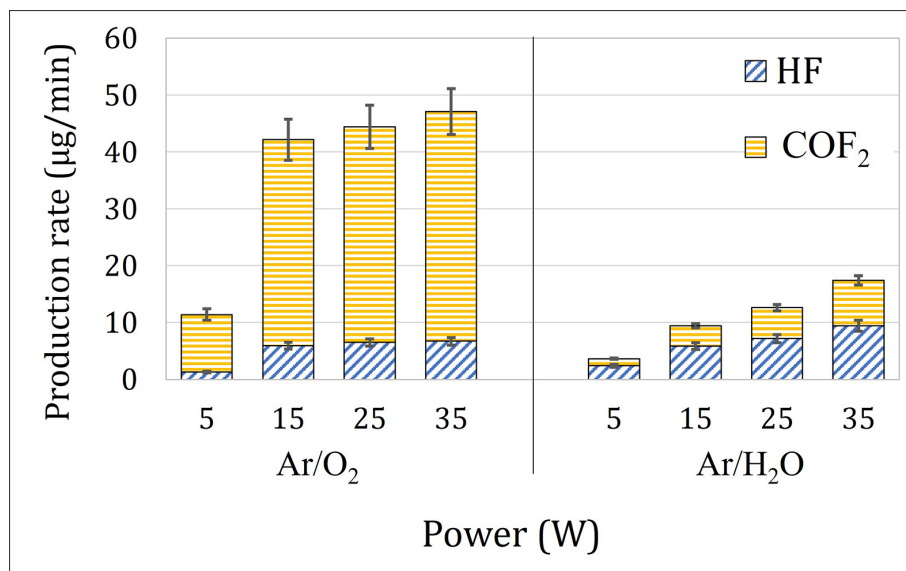


FIG. 6: Production of fluorinated molecules through the action of plasma on a PTFE tube in a 1.5 L/min Ar/O_2 and $\text{Ar}/\text{H}_2\text{O}$ gas mixture and the impact of power on that impact

15 W, with 47 $\mu\text{g}/\text{min}$, it reaches a threshold, with a production rate stabilizing around 45 $\mu\text{g}/\text{min}$.

Conversely, in the same condition, $\text{Ar}/\text{H}_2\text{O}$ plasma has fewer damaging properties and a slowly increased impact of the power on the degradation going from 4 $\mu\text{g}/\text{min}$ at 5 W to 9 $\mu\text{g}/\text{min}$ at 15 W. At 25 W, the degradation rate is off 13 $\mu\text{g}/\text{min}$ to finally reach 18 $\mu\text{g}/\text{min}$ at 35 W. The power range investigated here did not reach a degradation threshold for the $\text{Ar}/\text{H}_2\text{O}$ plasma.

A monolayer of PTFE in the 1.5 m PTFE tube was calculated to be 6 μg roughly. That means that for the harshest treatment (Ar/O_2), approximately seven layers are destroyed every minute. As for the 15W $\text{Ar}/\text{H}_2\text{O}$ plasma, it is approximately one layer every minute of treatment. To give perspective, it also means that it would take almost ten years of permanent $\text{Ar}/\text{H}_2\text{O}$ plasma to destroy a 1 mm thick PTFE tube.

C. Surface Analysis

1. AFM

The roughness of the surfaces of the PTFE film samples was investigated through AFM measurements. Plasma treatments on polymer can lead to etching and a change in the roughness of its surface. For different plasma gases, the PTFE surfaces exhibit different roughness. Figure 7 shows the R_q measured for each of these surfaces after 30 min of treatment with the different gas mixtures at 15 W (Fig. 7A), the impact of power in the case of $\text{Ar}/\text{H}_2\text{O}$ plasma (Fig. 7B) as well as the impact of time for $\text{Ar}/\text{H}_2\text{O}$ plasma (Fig. 7C) with the corresponding images (Fig. 7A to 7D). Figure 7A shows that for an applied power of 15 W, the Ar/O_2 plasma exhibits the highest roughness of all the gas mixtures. The $\text{Ar}/\text{H}_2\text{O}$ and air plasma also exhibit a significant roughness increase compared to the pristine sample (blank). Pure noble gas (argon and helium) showed little to no roughness modification compared to the pristine sample. Pure noble gas plasma, especially helium, is known to produce very highly energetic species that can destroy PTFE surface on a layer-to-layer mechanism, and so not influence the roughness.²³

A closer investigation of $\text{Ar}/\text{H}_2\text{O}$ was done. In Fig. 7B, the influence of the power is studied with variation between 5, 15, and 30 W at a fixed time of 30 min. It shows an increase in the roughness of the tube's surfaces with the power. Plasma at 5 W has a lower impact than higher-power plasma. The roughness does not increase between 15 W and 30 W. Variation of treatment time with a fixed power of 15 W was researched with time of 30 s, 1, 2, 5, 10, 30, and 60 min (Fig. 7C). A small increase of the surface roughness is seen at increased treatment time, going from 102 nm to 130. However, after an initial increase at the smallest treatment time (30 s), the roughness stabilizes at an average of 110 ± 12 nm, and longer treatment does not significantly increase the roughness.

Figure 8 (top) shows that the roughness analysis over treatment power has been performed for an Ar/O_2 in similar conditions to the $\text{Ar}/\text{H}_2\text{O}$ measurement. The associated AFM images of the sample before and after treatment are also displayed on the right. The 5 W treatment causes a small increase in the roughness of the PTFE surface, but it

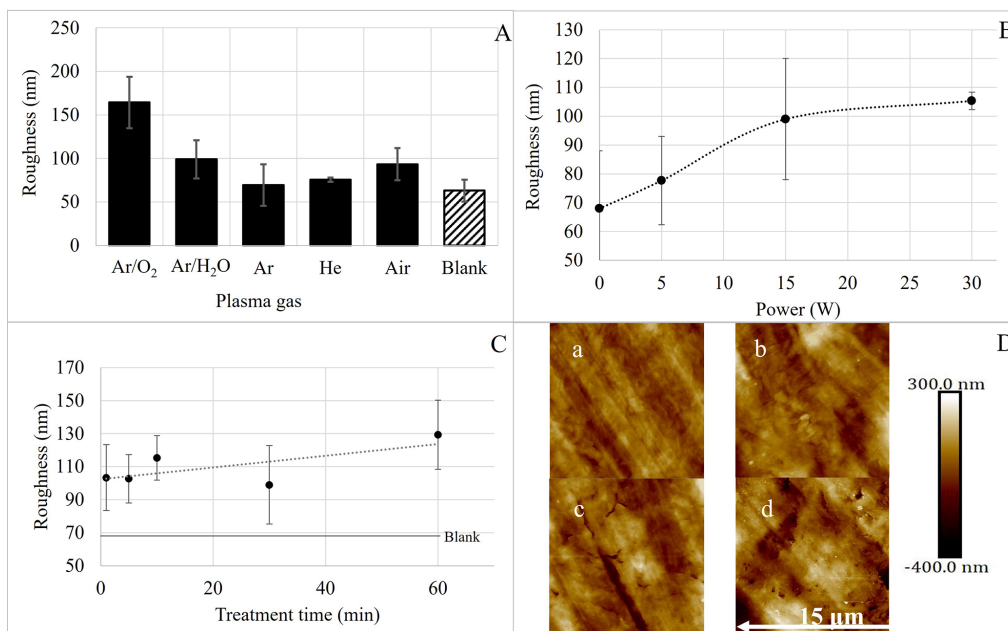


FIG. 7: (A) Influence of the gas of a 15 W 30 min plasma on the roughness of the surface of PTFE. (B) Influence of power with a 30 min Ar/H₂O. (C) Influence of treatment time with a 15 W Ar/H₂O plasma. (D) AFM images of PTFE surfaces after a 15 W plasma, Ar/H₂O. For (A), 0 min of plasma; (B), 1 min of plasma; (C), 10 min of plasma; and (D), 30 min of plasma.

is not significant. However, a significant increase is made by the 15 W plasma. As power is increased to 30 W, the measured roughness decreases. This could be explained by the semi-crystallinity of PTFE. Indeed, a 15 W Ar/O₂ plasma provides enough energy-rich species to affect the amorphous part of PTFE but not the crystalline parts, and doing so, increases the roughness by preferentially digging the surface. Conversely, the species produced by the 30 W plasma are energetic enough to affect both amorphous and crystalline parts, resulting in a more homogenous attack of the PTFE surface. The preferential degradation of amorphous parts over crystalline parts in plasma treatment of PTFE is a documented mechanism. Dufour et al. showed a similar mechanism in the case of He and He/O₂ post-discharged plasma.^{23,24} This mechanism is schematized in Figure 8 (bottom), which shows how the preferential attack of the amorphous phase at 15 W increases the roughness of the surface.

2. XPS

X-ray photoelectron spectroscopy (XPS) survey and high-resolution (HR) spectra were collected to analyze the chemical composition of the treated PTFE surface. In this study, the surface composition and surface chemistry of all samples, except for the He treatment, remained unaffected by the plasma conditions, as indicated by a constant F/C ratio

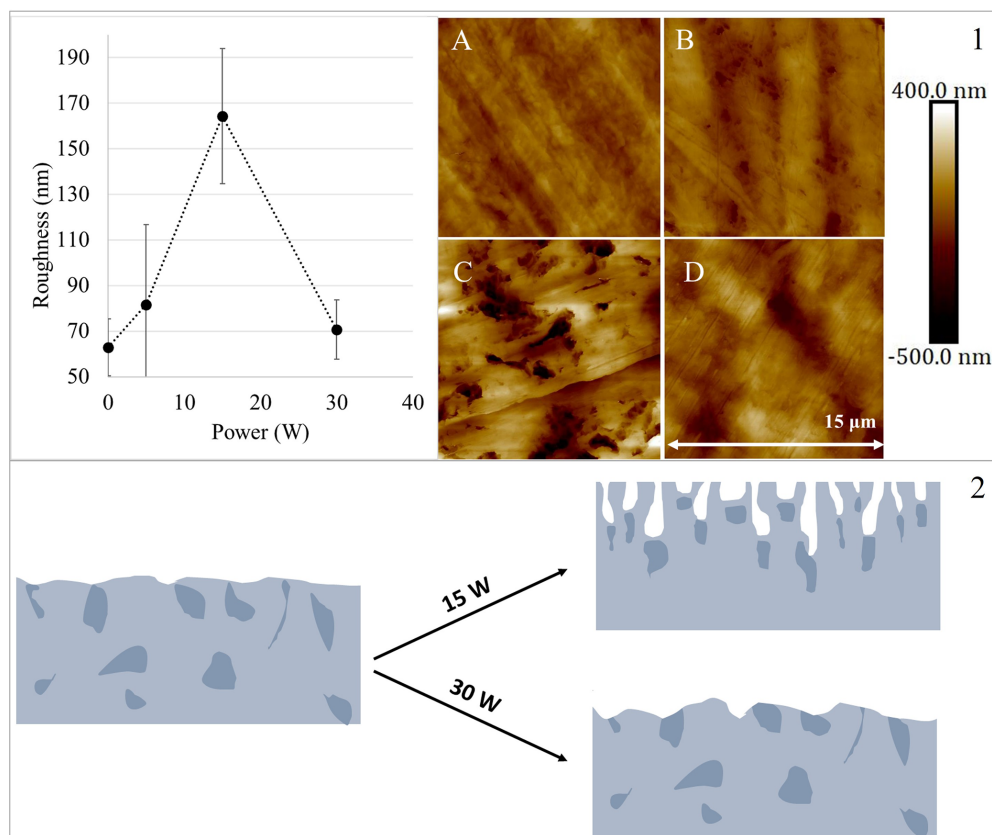


FIG. 8: (1) Influence of power on a 30 min Ar/O₂ plasma. (A) 0 W. (B) 5 W. (C) 15 W. (D) 30 W. (2) Schematic representation of the roughness of the PTFE surface before and after a 30 min Ar/O₂ plasma.

(Fig. 9), and an unchanged spectral envelope of the HR C 1s spectra following plasma exposure (not displayed). However, the survey and HR C 1s XPS spectrum for samples treated with pure helium plasma revealed the presence of oxygenated compounds, consistent with other observations in the literature.^{37,38} It also shows defluorination with decreased fluorine on the PTFE surface (Fig. 9A). The high energy of helium metastables has a critical role in the defluorination process. For all treatments, except helium, there were no major modifications in surface composition, although changes in surface wettability were observed. 1–2% of oxygen (O 1s) was found on the surface of Ar/H₂O treated samples. Grafted oxygen, even in small quantities, has been shown to increase the hydrophilicity of surfaces.

3. WCA

WCA measurements were carried out to characterize the evolution of the wettability of the PTFE after treatment with various gases (Fig. 10C), and in the case of Ar/O₂ and Ar/

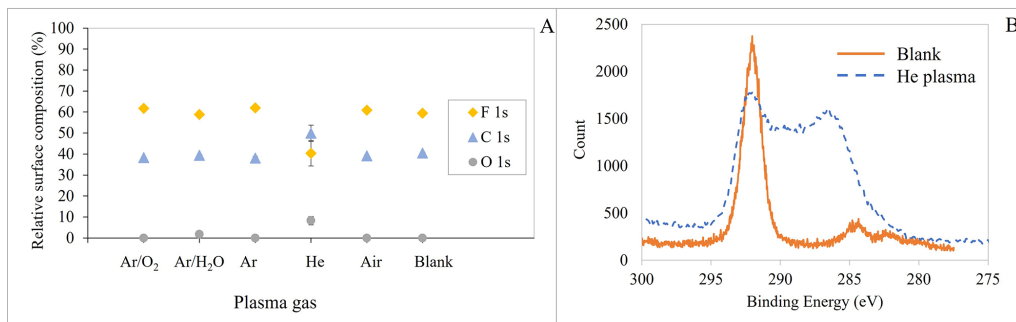


FIG. 9: (A) Atomic composition of treated PTFE samples after 30 min of a 15 W plasma. (B) HR spectra of 1 s of blank PTFE and PTFE treated with a 30 min, 15 W helium plasma.

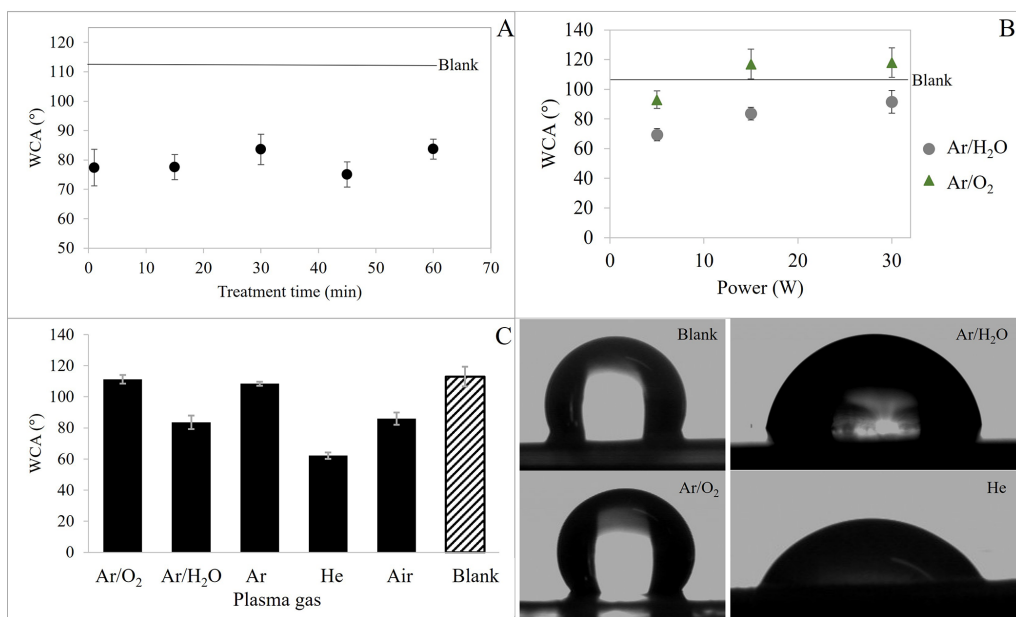


FIG. 10: Water contact angle of plasma-treated PTFE samples. (A) Over treatment time for a 15 W, Ar/H₂O plasma. (B) Over power for a 30 min treated Ar/H₂O and Ar/O₂ plasma. (C) Over various gases for 30 min at 15 W treatments.

H₂O, the influence of the treatment time (Fig. 10A), and/or plasma power (Fig. 10B). As reported in the literature, helium plasma decreases the WCA, which is confirmed in those measurements, going from 113° for blank PTFE to 62° after a 30-minute treatment at 15 W. This is consistent with the oxygen grafted at its surface observed with the XPS measurements. Small amounts of oxygen grafted with the Ar/H₂O plasma also affected the surface, with WCA decreasing to 84° after treatment. Pure Ar plasma treatment induces no modification of the wettability. It also showed no alteration in its chemical and

topographic properties. As some degradation was seen with the gas IRRAS measurement, it appears that the Ar plasma treatment removes a uniform layer of the PTFE without changing its surface properties.

In the cases of Ar/O₂ and Ar/H₂O treatment at low power (5 W), both samples show a decrease in the WCA relative to the blank sample. They both exhibit drastic diminution of hydrophobicity properties down to 69° for Ar/H₂O and 93° for Ar/O₂. On the contrary, at 15 W and 30 W, the treatment showed a lower decrease in the case of Ar/H₂O (84° and 92° respectively), and even increase compared to the blank sample for Ar/O₂ (117° and 118° respectively). For Ar/H₂O, this lower decrease in WCA can be related to the increased roughness observed by AFM. On the contrary, the Ar/O₂ samples treated at 15 W and 30 W exhibit higher hydrophobic properties relative to the blank sample, with a WCA of 118°. This behavior is correlated to the absence of oxygen grafting on the surface (XPS) and the increased roughness at least at 15 W.

IV. CONCLUSIONS

In this study, we examined the effects of plasma on the internal surface of tubular structures, particularly focusing on the case of the decontamination of endoscopes using CAP. CAP presents an innovative and promising method for addressing the modern and urgent challenge of endoscope decontamination. Our research targeted the implementation of CAP for cleaning long tubular structures and assessed its impact on the material of the tubes.

Our findings demonstrate that CAP is a realistic and feasible solution for decontaminating endoscopes. However, depending on the parameters used, the plasma treatment resulted in minor damage and surface modifications to the tubes. Notably, the Ar/O₂ mix showed the most significant degradation and surface modification, while the Ar/H₂O mix exhibited little degradation but increased surface roughness and decreased hydrophobicity. For the actual decontamination process, we opted for the Ar/H₂O mix as it gave the most promising results in terms of bactericidal effect and biofilm destruction in our setup (the decontamination treatment is discussed in a separate work).³⁰

Further analysis is necessary to determine whether these changes affect biofilm growth or the antifouling properties of PTFE. Currently, there is limited information on the impact of existing cleaning processes on endoscopes, preventing a direct comparison with our method. Nonetheless, our study offers a detailed and conservative understanding of the effects of plasma decontamination, with potential applications extending to a wide range of medical devices that rely on surface properties for their functionality.

ACKNOWLEDGMENTS

This research was supported by the Université Libre de Bruxelles, with the funding of the ARC project - COSMIC. The authors would also like to thank David Petitjean for his technical support. The Jaumotte-Demoulin Foundation also provided financial

support allowing the XPS analysis. The research at LPNE (UMONS) is partly supported by F.R.S. FNRS (Belgium) via the Grands Equipements Project (40007941) – 2022 “Interuniversity Platform for the Analysis of the Nanoscale Properties of Emerging Materials and their Applications (IPANEMA).”

REFERENCES

1. Beilenhoff U, Biering H, Blum R, Brljak J, Cimbri M, Dumonceau J-M, Hassan C, Jung M, Neumann C, Pietsch M, Pineau L, Ponchon T, Rejchrt S, Rey J-F, Schmidt V, Tillett J, Hooft J van. Prevention of multidrug-resistant infections from contaminated duodenoscopes: Position statement of the European Society of Gastrointestinal Endoscopy (ESGE) and European Society of Gastroenterology Nurses and Associates (ESGENA). *Endoscopy*. 2017;49(11):1098–106.
2. Rutala WA, Weber DJ. Gastrointestinal endoscopes: A need to shift from disinfection to sterilization? *JAMA*. 2014;312(14):1405–6.
3. Rutala WA, Weber DJ. Guideline for disinfection and sterilization of prion-contaminated medical instruments. *Infection Control Hospital Epidemiol*. 2010;31(2):107.
4. Helmke A, Gerling T, Weltmann KD. Plasma sources for biomedical applications. In: Metelmann HR, von Woedtke T, Weltmann, KD, editors. *Comprehensive clinical plasma medicine: Cold physical plasma for medical application*. Cham, Switzerland: Springer International Publishing; 2018. p. 23–41.
5. Bazaka K, Jacob MV, Crawford RJ, Ivanova EP. Plasma-assisted surface modification of organic biopolymers to prevent bacterial attachment. *Acta Biomaterialia*. 2011;7(5):2015–28.
6. Nikiforov A, Deng X, Xiong Q, Cvelbar U, DeGeyter N, Morent R, Leys C. Non-thermal plasma technology for the development of antimicrobial surfaces: A review. *J Phys D Appl Phys*. 2016;49(20):204002.
7. Rossi F, Kylián O, Rauscher H, Gilliland D, Sirghi L. Use of a low-pressure plasma discharge for the decontamination and sterilization of medical devices. *Pure Appl Chem*. 2008;80(9):1939–51.
8. Tanaka H, Ishikawa K, Mizuno M, Toyokuni S, Kajiyama H, Kikkawa F, Metelmann H-R, Hori M. State of the art in medical applications using non-thermal atmospheric pressure plasma. *Rev Mod Plasma Phys*. 2017;1(1):3.
9. von Woedtke T, Reuter S, Masur K, Weltmann K-D. Plasmas for medicine. *Phys Rep*. 2013;530(4):291–20.
10. Dang CN, Anwar R, Thomas G, Prasad YDM, Boulton AJM, Malik RA. The Biogun: A novel way of eradicating methicillin-resistant *Staphylococcus aureus* colonization in diabetic foot ulcers. *Diabetes Care*. 2006;29(5):1176.
11. Morent R, Geyter ND, Morent R, Geyter ND. Inactivation of bacteria by non-thermal plasmas. In *Biomedical Engineering - Frontiers and Challenges*. IntechOpen; 2011. doi: 10.5772/18610.
12. Ikawa S, Kitano K, Hamaguchi S. Effects of pH on bacterial inactivation in aqueous solutions due to low-temperature atmospheric pressure plasma application. *Plasma Process Polym*. 2010;7(1):33–42.
13. Giannetti E. Semi-crystalline fluorinated polymers. *Polym Int*. 2001;50(1):10–26.
14. Zhu Y, Yu S, Zhang B, Li J, Zhao D, Gu Z, Gong C, Liu G. Antifouling performance of polytetrafluoroethylene and polyvinylidene fluoride ultrafiltration membranes during alkali/surfactant/polymer flooding wastewater treatment: Distinctions and mechanisms. *Sci Total Environ*. 2018;642:988–98.
15. Donnelly B, Sammut K, Tang Y. Materials selection for antifouling systems in marine structures. *Molecules*. 2022;27(11):3408.
16. Cassidy AI, Hidzir NM, Grøndahl L. Enhancing expanded poly(tetrafluoroethylene) (ePTFE) for biomaterials applications. *J Appl Polym Sci*. 2014;131(15):40533.
17. Guillén-Burrieza E, Thomas R, Mansoor B, Johnson D, Hilal N, Arafat H. Effect of dry-out on the

- fouling of PVDF and PTFE membranes under conditions simulating intermittent seawater membrane distillation (SWMD). *J Membr Sci.* 2013;438:126–39.
18. Kim SR. Surface modification of poly(tetrafluoroethylene) film by chemical etching, plasma, and ion beam treatments. *J Appl Polym Sci.* 2000;77(9):1913–20.
 19. Liu C, Cui N, Brown NMD, Meenan BJ. Effects of DBD plasma operating parameters on the polymer surface modification. *Surf Coat Tech.* 2004;185(2):311–20.
 20. Sarani A, De Geyter N, Nikiforov A Yu, Morent R, Leys C, Hubert J, Reniers F. Surface modification of PTFE using an atmospheric pressure plasma jet in argon and argon+CO₂. *Surf Coat Tech.* 2012;206(8):2226–32.
 21. Liu C, Arnell RD, Gibbons AR, Green SM, Ren L, Tong J. Surface modification of PTFE by plasma treatment. *Surf Eng.* 2000;16(3):215–7.
 22. Liu CZ, Wu JQ, Ren LQ, Tong J, Li JQ, Cui N, Brown NMD, Meenan BJ. Comparative study on the effect of RF and DBD plasma treatment on PTFE surface modification. *Mater Chem Phys.* 2004;85(2):340–6.
 23. Hubert J, Dufour T, Vandecasteele N, Desbief S, Lazzaroni R, Reniers F. Etching processes of polytetrafluoroethylene surfaces exposed to He and He–O₂ atmospheric post-discharges. *Langmuir.* 2012;28:9466–74.
 24. Dufour T, Hubert J, Vandecasteele N, Viville P, Lazzaroni R, Reniers F. Competitive and synergistic effects between excimer VUV radiation and O radicals on the etching mechanisms of polyethylene and fluoropolymer surfaces treated by atmospheric He–O₂ post-discharge. *J Phys D: Appl Phys.* 2013;46:315203.
 25. Dufour T, Hubert J, Viville P, Duluard CY, Desbief S, Lazzaroni R, Reniers F. PTFE surface etching in the post-discharge of a scanning RF plasma torch: Evidence of ejected fluorinated species. *Plasma Process Polym.* 2012;9:820–9.
 26. Al-Amshawee S, Yunus MYBM, Lynam JG, Lee WH, Dai F, Dakhil IH. Roughness and wettability of biofilm carriers: A systematic review. *Environ Technol Innov.* 2021;21:101233.
 27. Hoevels J, Lunderquist A, Owman T, Ihse I. A large-bore teflon endoprosthesis with side holes for nonoperative decompression of the biliary tract in malignant obstructive jaundice. *Gastrointest Radiol.* 1980;5(1):361–6.
 28. Tariq M, Youseffi M, Jamil M, Abd Rahman NA, Khaghani SA, Sefat F. A study on the application of convoluted PTFE for arterial implantation: Mechanical testing and properties. *J Physics: Conference Series.* 2020;1529:052032.
 29. Bhise O, Ravishankar S. “Modeling mechanical behavior of polytetrafluoroethylene tubes,” 2017. SAE Technical Paper 2017-26-0279.
 30. Remy A, Nonclercq A, Zveny J. Pseudomonas aeruginosa biofilm decontamination and removal by Ar/H₂O cold atmospheric plasma in endoscope-like tubing. In press 2024.
 31. Bastin O, Thulliez M, Servais J, Nonclercq A, Delchambre A, Hadeff A, Devière J, Reniers F. Optical and electrical characteristics of an endoscopic DBD plasma jet. *Plasma Med.* 2020;10(2):415204.
 32. Thulliez M, Bastin O, Remy A, Nonclercq A, Devière J, Delchambre A, Reniers F. Effect of gas flow on a helium/oxygen endoscopic plasma jet. *J Phys D Appl Phys.* 2022;55(41):415202.
 33. Rothman LS, Gordon IE, Babikov Y, Barbe A, Chris Benner D, Bernath PF, Birk M, Bizzocchi L, Boudon V, Brown LR, Campargue A, Chance K, Cohen EA, Coudert LH, Devi VM, Drouin BJ, Fayt A, Flaud J-M, Gamache RR, Harrison JJ, Hartmann J-M, Hill C, Hodges JT, Jacquemart D, Jolly A, Lamouroux J, Le Roy RJ, Li G, Long DA, Lyulin OM, Mackie CJ, Massie ST, Mikhailenko S, Müller HSP, Naumenko OV, Nikitin AV, Orphal J, Perevalov V, Perrin A, Polovtseva ER, Richard C, Smith MAH, Starikova E, Sung K, Tashkun S, Tennyson J, Toon GC, Tyuterev VI G, Wagner G. The HITRAN2012 molecular spectroscopic database. *J Quant Spectrosc Radiat Transf.* 2013;130:4–50.

34. Bhatt S, Mehta P, Chen C, Schneider CL, White LN, Chen H-L, Kong MG. Efficacy of low-temperature plasma-activated gas disinfection against biofilm on contaminated GI endoscope channels. *Gastrointest Endosc.* 2019;89(1):105–14.
35. Sato T, Furuya O, Ikeda K, Nakatani T. Generation and transportation mechanisms of chemically active species by dielectric barrier discharge in a tube for catheter sterilization. *Plasma Process Polym.* 2008;5(6):606–14.
36. Sarani A, Nikiforov AY, Leys C. Atmospheric pressure plasma jet in Ar and Ar/H₂O mixtures: Optical emission spectroscopy and temperature measurements. *Phys Plasmas.* 2010;17(6):063504.
37. Tanaka K, Kogoma M. Investigation of a new reactant for fluorinated polymer surface treatments with atmospheric pressure glow plasma to improve the adhesive strength. *Int J Adhes Adhes.* 2003;23(6):515–9.
38. Zettsu N, Itoh H, Yamamura K. Plasma-chemical surface functionalization of flexible substrates at atmospheric pressure. *Thin Solid Films.* 2008;516(19):6683–7.